ARCHIVES OF ELECTRICAL ENGINEERING VOL. 65(4), pp. 671-683 (2016)

DOI 10.1515/aee-2016-0047

Magnet loss analysis for a high-speed PM machine with segmented PM and modified tooth-tips shape

ADRIAN MLOT[1], MARIAN ŁUKANISZYN[1], MARIUSZ KORKOSZ[2]

[1] *Opole University of Technology*
Faculty of Electrical Engineering, Automatic Control and Informatics
Gen. K. Sosnkowskiego 31, 45-758 Opole
e-mail: a.mlot@po.opole.pl, m.lukaniszyn@po.opole.pl

[2] *Rzeszow Univeristy of Technology*
Faculty of Electrical and Computer Engineering
W. Pola 2, 35-959 Rzeszow
e-mail: mkosz@prz.edu.pl

(Received: 16.10.2015, revised: 29.08.2016)

Abstract: This paper presents the loss-oriented performance analysis of a radial high-speed permanent magnet (PM) machine with concentrated windings for automotive application. The PM synchronous machine was designed for an operating frequency up to 800 Hz. The main aim of this paper is to analyse the selected methods for magnet eddy-current loss reduction. The first approach to rotor modification regards magnet segmentation in circumferential and axial directions. The second approach is based on changes in tooth-tips shape of the stator. The best variants of tooth-tip shapes are determined for further investigation, and adopted with a rotor having magnet segmentation. It is found that the machine with a segmented magnet leads to magnet loss reduction by 81%. Further loss reduction by 45% can be realized with the proposed tooth-tip shape. Additionally, owing to the stator and rotor modifications, the main machine parameters are investigated, such as back-EMF, electromagnetic torque, torque ripple and cogging torque. The 2-D and 3-D finite element analysis (FEA) is used for electromagnetic analysis. An experimental approach based on a partially wound stator is employed to verify the 3-D FEA.

Key words: magnet loss reduction, magnet segmentation, tooth-tip modification, permanent magnet machine, high-speed motor

1. Introduction

Permanent magnet synchronous brushless machines (PMSM) having a high power density and good dynamic performance are widely used in many industries [1-6]. High-speed, large size PMSM in the bus, military vehicle and truck units require from engineers focusing on the machine having light weight, high-performance, high efficiency and fuel reduction units with an appropriate level of durability. Vehicles with large size and large weight used in transport/ military sectors require high quantity of torque and power. In this case the radial-flux PMSM

would be easily integrated into the huge vehicle. The axial-flux technology to pack more torque and power into a smaller, lighter unit is already developed by prominent industry and it seems the perfect solution for many pure EVs and HEVs applications [7]. Both radial and axial machines are operating at high-speed in the automotive application. In this case the eddy-current (EC) loss in the magnet can be extremely significant. It is a major problem in the electric machine operating at high-speed, especially in large size. This loss has to be properly understood for designing of the rotor and stator [8]. The EC loss distribution in PMs has recently attracted more attention for electrical machines used for automotive applications [9-12]. Less attention has been paid to an alternative method for magnet segmentation [13-15]. Some of these methods based on modified stator and rotor shapes are developed mostly for interior PM motors in order to reduce the magnet EC loss [16, 17].

The purpose of this paper is to investigate a number of EC loss minimization techniques in the radial-flux PMSM machine with exterior mounted magnets onto the rotor. In the first stage, the magnet EC loss reduction is approached by magnet segmentation in both circumferential and axial directions. Those techniques are commonly used to improve the performance of PMSM [10-13]. Next, the interest is to analyse the EC loss that can be reduced by modified stator tooth-tips. It will be interesting to do further investigation of EC loss analysis by adopting both techniques: a segmented magnet and modified tooth-tip shape.

This study concerns the design of a compact (2 kW/kg continuous rated) water jacket cooled PMSM for a large-size vehicle traction application. 2-D and 3-D modeling of the PMSM with respect to the electromagnetic numerical simulations of motor performance, electromagnetic torque and magnet loss are presented. The FE model is also validated by a number of experimental tests of AC loss at high frequency operation.

2. FEA validation

2.1. Prototype motor definition and test rig

The founding of high-speed 3-phase PMSM comprises an 8-pole rotor with solid magnets mounted onto the rotor and that leads consequently to a high operating frequency up to 800 Hz. The 12-slot laminated stator is made of 0.35 mm silicon iron with a double layer concentrated winding. The main machine parameters are given in Table 1.

Table 1. The reference machine definition

Parameter	Value
Stator inner/outer radius (mm)	87.5/145
Slot height (mm)	35
Stator/rotor yoke height (mm)	17/13
Magnet height (mm)	10
Magnet pole pitch (el. deg.)	147
Machine length (mm)	250
Stator core and magnet material	M300-35 A / N33 EH

Fig. 1a shows a cross section of the mathematical model (3-D FEM) of the PMSM with the winding sequence U+/V+/W+ used for PM loss and motor performance analysis. The model comprises the standard tooth-tip shape. For thermal tests and to evaluate the power loss within the analysed machine a simplified approach has been adopted utilizing the segmented stator topology. A three-tooth sector of the stator with a single wound coil surrounded by unwound segments can be used to provide valuable data for both theoretical and experimental validations, Figs. 1b-c. Fig. 1c shows three segments of the stator mounted on a cold plane cooled via an outer water jacket and set up in the environmental chamber. To simplify the analysis, the influence of the rotor and the mutual coupling between phases are assumed to be negligible.

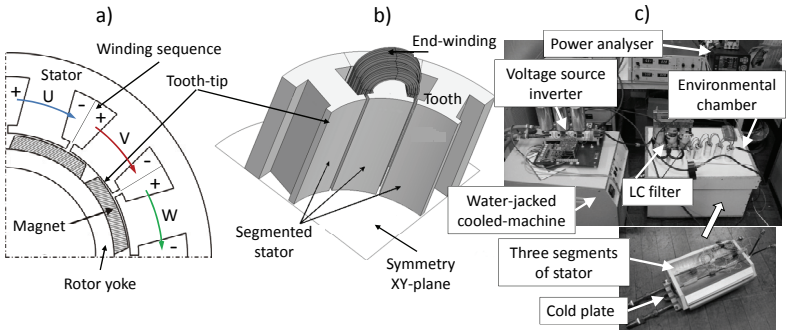

Fig. 1. Cross-section of the PMSM with periodic solution domain (a), 3-D numerical model of a three tooth sector of the stator (b), used in the verification executed by experimental test (c)

2.2. Numerical analysis of the basic motor performance

To validate the FE model the theoretical investigation of AC loss is carried out using a 3-D FEA based on a steady state AC harmonic formulation, and takes into account the distribution of the eddy-current induced in the conducting regions. In the first stage of armature design the winding includes 14 turns with 7 parallel conductors within a bundle, used only for FE model validation. A single tooth winding is instrumented with a number of type-K thermocouples. Then temperature measurements are monitored at each side of the coil including active length and end-windings. The thermal steady state is defined as temperature changes less than 1°C over 10 min. And the maximum recorded copper temperature was selected in the numerical model for the entire winding. The example of the temperature recorded for winding at I = 40 A is depicted in Fig. 2b. A number of tests were carried out to assess the power loss generated within the setup under AC operation. The winding was energised with the sinusoidal current of 40 A at 400/600/800 Hz. AC loss predictions including both a winding and laminated stator are compared with measurements giving a good agreement, Fig. 2a. The error of the AC measurements and 3-D FEA can be caused by geometry precision of the numerical model according to the winding strands, air-gap between stator segments, and the end-winding shape.

At 100 A the temperature of copper at 800 Hz reached very quickly 153°C (Fig. 2). The maximum variable frequency sinusoidal current is assumed to be 150 A. Then the wire may

start to overheat substantially, therefore, the 15 AWG wire size is proposed to be used. This leads to increase in the number of parallel conductors from 7 to 14 for RMS copper current density limitation. Then the number of turns per coil was reduced from 14 to 9. And that a new coil is finally used to the numerical model with a 50% copper fill factor, Fig. 1a. Due to both rotational and XY-plane symmetries only the 1/8 section of the complete motor cross-section needs to be modeled, Fig. 1a.

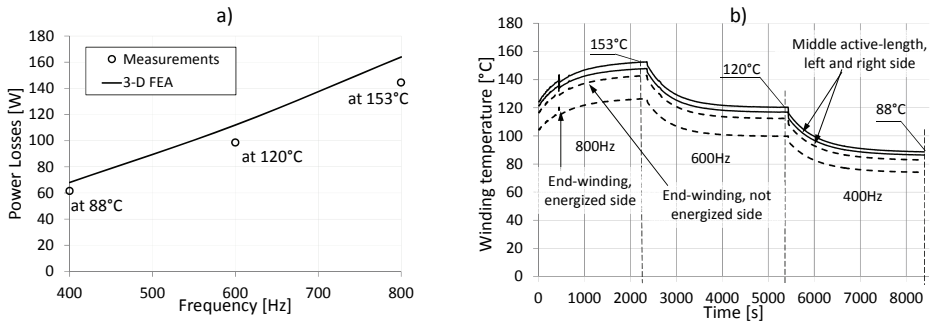

Fig. 2. Experimental power loss with the numerical 3-D FEA (a) and winding temperature recorded (b) for 14-turn winding with 7 parallel bonded conductors (copper, ø1.60 mm)

Small changes in geometry dimensions can cause remarkable differences in the resulting performance of large PMSM. In this paper we focus on the EC loss in the PMs and torque computation for the machine with modified stator and rotor. Electromagnetic torque (T_e) is based on the stored magnetic co-energy change ($W_{co\text{-}eng}$) or the virtual work with a small displacement at constant current (I).

$$T_e = \left.\frac{\Delta W_{co-eng}}{\Delta\theta}\right|_{I=\text{const}}. \tag{1}$$

EC loss generated in the PMs mainly arises from the flux density variations due to the stator slot opening and MMF time harmonics. The last cause of EC loss is not considered in this study since pure sinusoidal phase current excitation is assumed (high-frequency PWM effects neglected). In this paper the Joule loss of PMs is computed by FEA at 20°C and is expressed as:

$$W_{PM} = \iiint_V \boldsymbol{E}\cdot\boldsymbol{J}\,\mathrm{d}V = \rho\iiint_V \boldsymbol{J}^2\,\mathrm{d}V, \tag{2}$$

where: $\boldsymbol{E}$ is an electric field strength, $\boldsymbol{J}$ is the current density in the PM, ρ is the resistivity of the PM (180 μΩcm), V is the PM volume.

Figs. 3a-b show the calculations of the electromagnetic torque curve (assuming the current in the phase A-B-C equal to $I_A = \sqrt{2}\cdot I$, $I_B = I_C = -\sqrt{2}\cdot I/2$) and cogging torque (I = 0 A) accomplished in the magneto-static application. The torque curve varies sinusoidally with the

mechanical angle for a fixed current in the stator, Fig. 3a. The torque ripples are mainly caused by cogging torque T_{cog} which is equal to 13.8 N m. Fig. 3c illustrates the variations in torque for the pure sinusoidal current waves.

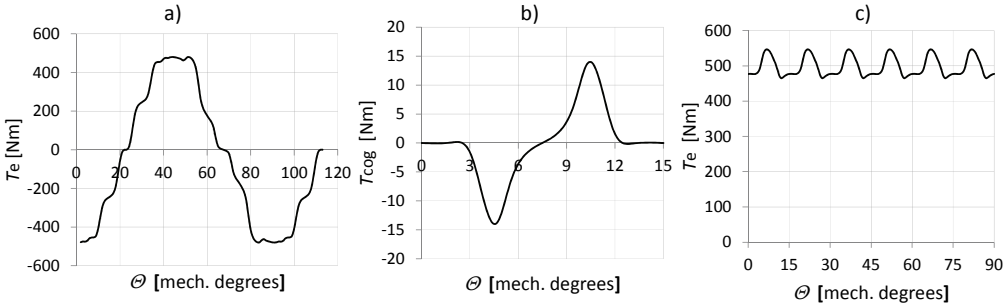

Fig. 3. Electromagnetic torque T_e for I = 150 A (a) and cogging torque T_{cog} (b) computed in magneto-static application, and variations of the torque for I = 150 A (c) vs. rotor mechanical position θ

Fig. 4a demonstrates the line-to-line back-EMF waveforms at open-circuit (OC) operation for n = 1000 r/min, which is below the base speed of the motor. At the same angular speed the current waveforms at short-circuit (SC) operation are depicted in Fig. 4b.

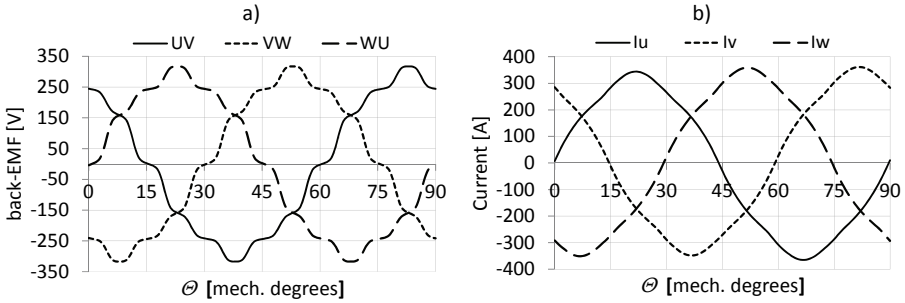

Fig. 4. Line-to-line back-EMF at open-circuit operation (a) and current waveforms at short-circuit operation (b) vs. rotor position θ at 1000 r/min

Fig. 5a shows the variation of the magnet loss W_{PM} at OC, SC and full load operation. Depending on motor speed the magnet loss at the SC operation is approximately three-four times higher than results at full load operation. It clearly shows that the PM eddy-current must be reduced to avoid the PM demagnetizing effect. It is important that the mover of the *PM* electric machine designed to produce required flux to reach the desired torque or induced voltage, cannot be demagnetized under periods of high load. Here, a critical typical scenario is a SC operation at an elevated temperature and full load operation. It is obvious that the high eddy-current in the PMs leads to rise the temperature in the magnets. And because the magnetic properties of NdFeB magnets are highly dependent on temperature, there is a high risk of partial/full demagnetisation at the event of the SC operation.

The overall EC loss in the solid magnets (n = 1) becomes considerably high at high speed, and generates up to 34.6 kW, 145 kW and 610 W at full load, three-phase symmetrical short-circuit and open-circuit conditions, respectively (Fig. 5b). And the loss leads to a rapid rise of the magnet temperature and degradation of the magnet performance. SC incidents on traction motors may have an adverse impact on vehicle stability. And SC operation can cause pulsating or even steady state braking torque in AC drives causing a sudden halt to the electric hybrid vehicle. For these reasons it is important to analyse PM loss at the SC condition.

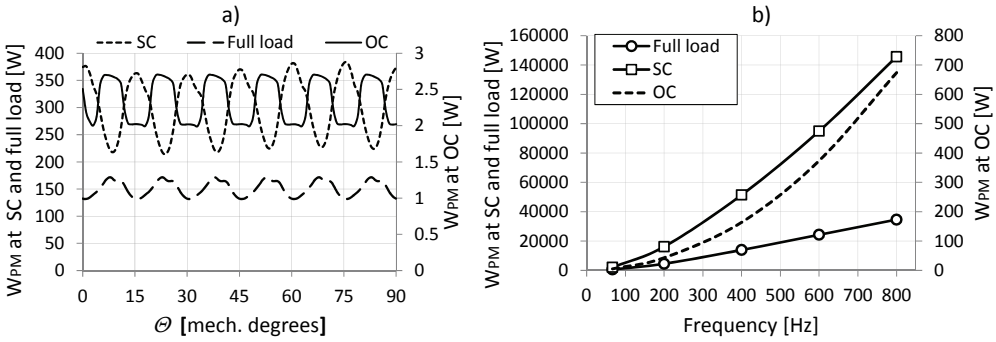

Fig. 5. Magnet loss W_{PM} in the solid magnet (no segmentation) under open-circuit, short-circuit and full load operation vs. rotor position θ (a) at 1000 r/min and vs. frequency (b)

3. The magnet EC loss minimization techniques and performance analysis

3.1. Magnet segmentation

The W_{PM} in the used sintered NdFeB magnet material is prominent as the magnets position is much closer to the stator. It can be easily concluded that changing air-gap distance between magnets may influence the magnet loss quantity. The proposed machine with a magnet radially and/or circumferentially segmented is comprehensively investigated by using 3-D FE models. The electrical insulation material of 0.1 mm width is set to each segment direction. The evaluated EC vectors on magnets with a rotor at *d*-axis at full load conditions are plotted in Fig. 6.

From Fig. 6a it is found that the W_{PM} loss at the surface of the magnet is extremely high when the PM is solid (no PMs segmentation). Fig. 6b shows an example of one pair pole of the rotor, where the magnet is divided into n = 5 pieces in the circumferential direction. Fig. 6c shows an example where each magnet is subdivided into n = 16 pieces along the axial length. And both segmentation methods adopted to prevent the EC are presented in Fig. 6d. The effect of division of the magnet on the EC loss demonstrates the change in the EC paths in the magnet. It is clarified that the EC loss decrease strongly as the number of division of magnet n increases. It is quantitatively clarified that the divided magnet is very useful to decrease EC loss in PMSM with surface mounted magnet.

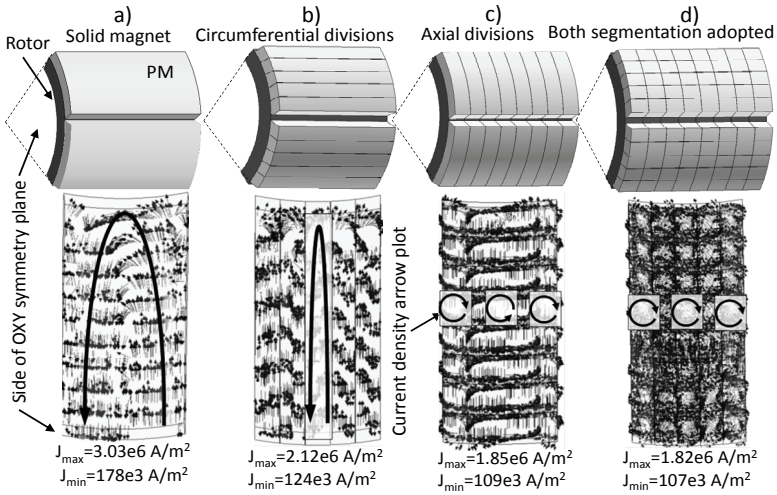

Fig. 6. EC vector and density on PMs at full load operation (I = 150 A, f = 800 Hz) with segmentation definitions: solid magnet (a), n = 5 in circumferential direction (b), n = 16 in axial direction (c), and both segmentation with 5 and 16 magnet segments in circumferential and axial directions respectively (d)

The corresponding W_{PM} loss in the magnet with different numbers of magnet segments under SC and OC conditions at 1000 r/min are analysed in this study. The effect of the number of the division n on the EC is depicted in Figs. 7a-c.

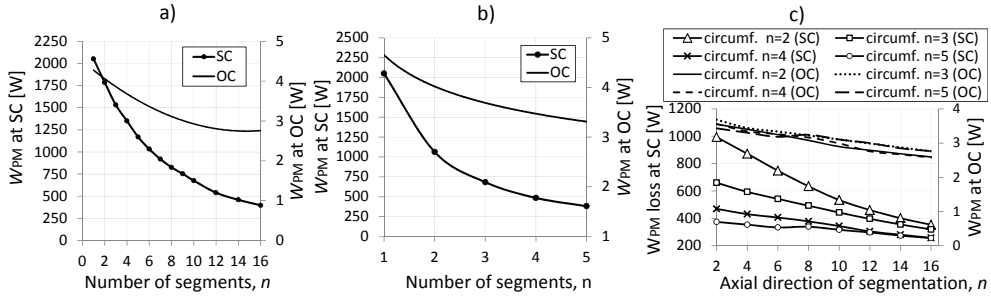

Fig. 7. EC loss in PM at 1 k rpm under SC and OC conditions. Segmented PM in circumferential direction (a), in axial direction (b), and both adopted methods of segmentation (c)

The W_{PM} loss for the proposed machine with 16 segments of the axial direction, and 5 segments of the circumferential direction at the SC condition are around 397 W and 380 W, respectively. And segmented magnets implemented to cut the paths of EC decreased the magnet loss about 81%. Further modification can be achieved when both circumferential and axial segmentations are adopted and the magnet loss was reduced to 255 W (n = 16 in axial direction and n = 5 in circumferential direction), Fig. 7c. Table 2 presents how much the main performance and efficiency of the machine is affected by magnet segmentation.

It is important to note that the values of torque constant k_T and voltage constant k_e are changed slightly by magnet segmentation. And because the PM loss was significantly reduced

the efficiency η of the motor increased, although the iron loss increased due to flux leakage caused by air-gaps between magnet segments. Also it can be seen that the short-circuit current was reduced and torque ripple coefficient ε was slightly increased [18].

The major problem of segmentation in the circumferential direction is that the mechanical strength of the magnet decreases when the number of segments *n* increases. Also, the magnet segmentation in the axial direction with a high number of division *n* can be expensive and more complex to assembly.

Table 2. Rotor design data for selected number of magnet segments at 1000 r/min

Motor version	W_{PM} [W]			P_{Fe} [W]			T_e [N·m]	ε [%]	k_T [N·m/A_{rms}]	I [A_{rms}]	k_e [V·s/rad]	η [-]
	SC	OC	Full load	SC	OC	Full load	Full load			SC	OC	
Ref. motor	2051	4.94	610	75	212	401	506	16.8	3.38	306	1.89	0.94
Axial $n = 16$	397	2.66	141	103	304	403	505	16.4	3.37	295	1.88	0.956
Circumf. $n = 5$	380	3.64	132	97	294	389	500	17.2	3.33	291	1.89	0.957
Axial $n = 16$ Circumf. $n = 5$	255	2.77	92	96	295	389	499	17.4	3.33	288	1.88	0.958

3.2. Modifying the tooth-tips of stator core

Fig. 8 presents the design variables for the selected stator tooth-tips. Since the motor is a radial-flux topology, 2-D FEA was used to calculate various versions of modified tooth-tips. At this study, non-segmented PM array constructions are considered only. Each tooth-tip version is carried out to determine the final shape for the maximum W_{PM} loss reduction without significant torque reduction. Versions I and II represent the modified tooth-tips at the corners with two variable parameters (α and *a*), Figs. 8a-b. In the second case when α increases, the radius (*R*) of tooth-tips increases as well and ranges from 2.6 mm to 17 mm. Versions III-IV and V-VI consist, single and double notches in the tooth-tips, respectively. Variable parameter of β_1 from version V is set to $\beta_1=\beta+1°$.

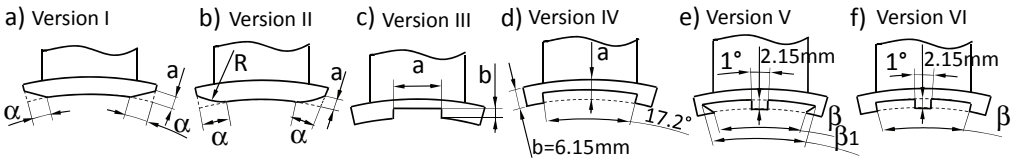

Fig. 8. Design variables at the top of stator tooth (tooth-tip)

In order to visualize the magnet EC loss versus tooth-tip design variables the FEA results of induced EC loss normalised by the magnet EC induced in the reference motor are shown in Fig. 9. Motor versions I and II lead to increase in the W_{PM} at load operation, and significantly reduce the W_{PM} loss at OC condition, Figs. 9a-b and Table 3. In the cases of motor versions III-VI the EC loss at load operation can be significantly reduced, Figs. 9c-f. For the motor version IV-VI the variable parameter a/b, β in the range of 0.2-0.45, 10°-17°, 16°-20°, respectively, lead to the smallest W_{PM}.

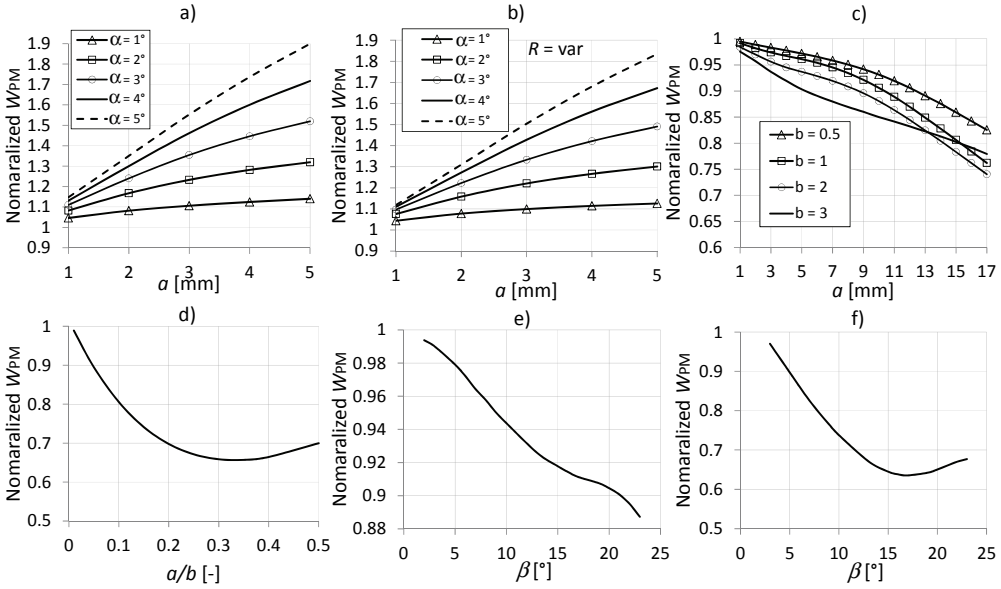

Fig. 9. The normalised magnet EC loss vs. tooth-tip design variables at 1000 r/min and full load 150 A. Motor version I (a), version II (b) version III (c), version IV (d), version V (e), and version VI (f)

Changing the design parameters of the tooth-tip shape leads to change in the vibration and noise caused by cogging torque and electromagnetic torque ripple. These changes can seriously affect the motor performance. Figs. 10 and Fig. 11 demonstrate the variation of the normalized cogging torque T_{cog} and torque constant k_T by the T_{cog} and k_T of the reference motor versus the tooth-tip design variables. All motor versions except the motor version IV lead to increase in the cogging torque.

The numerical findings suggest that motor versions III-VI show acceptable options for significant W_{PM} reduction and keeping the electromagnetic torque or torque constant k_T at reasonable levels at load operation, Figs. 11c-f and Figs. 9c-f.

Fig. 12 shows the variation in the voltage constant k_e normalised by the k_e of the reference motor versus tooth-tip design variables. The k_e is computed at open-circuit operation and it decreases in all tooth-tip design cases. Nevertheless, the motor versions III-VI show that the k_e reduction is relatively small compared with the huge reduction of the W_{PM}.

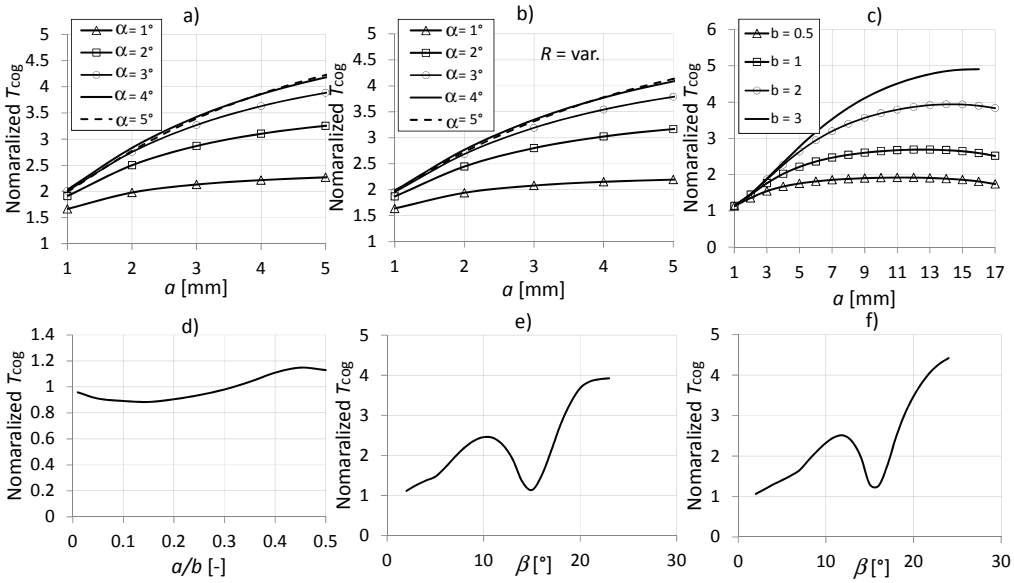

Fig. 10. The normalised amplitude of the cogging torque versus tooth-tip design variables. Motor version I (a), version II (b) version III (c), version IV (d), version V (e), and version VI (f)

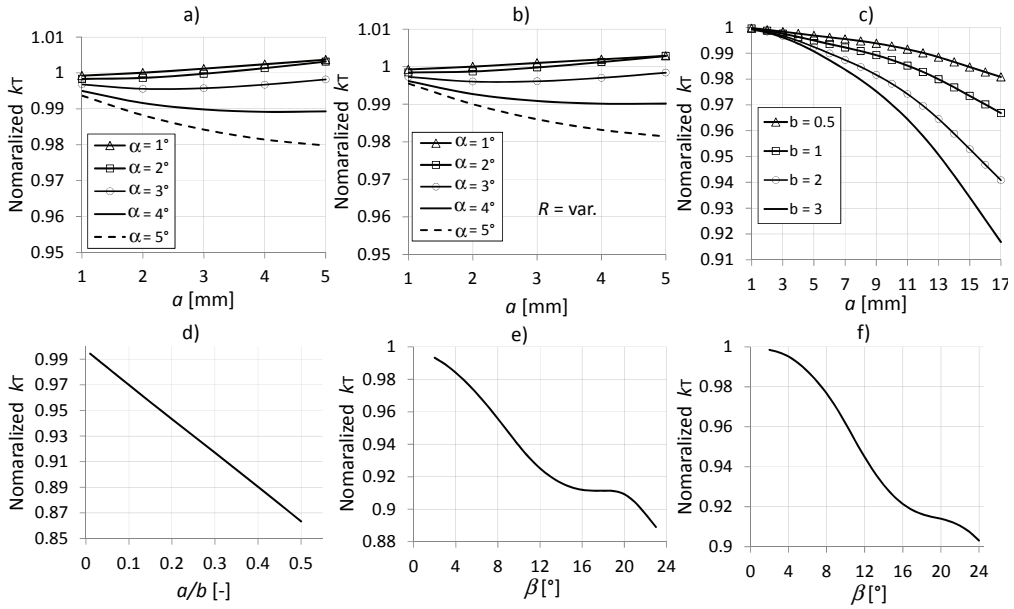

Fig. 11. The normalised k_T by the reference motor vs. tooth-tip design variables at 1000 r/min and full load. Motor version I (a), version II (b), version III (c), version IV (d), version V (e), and version VI (f)

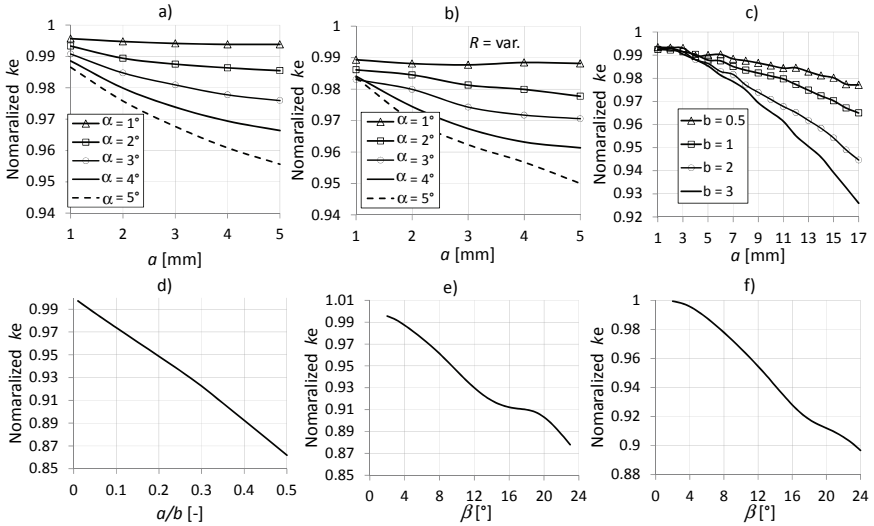

Fig. 12. The normalised k_e by the reference motor versus tooth-tip design variables at 1000 r/min and full load. Motor version I (a), version II (b) version III (c), version IV (d), version V (e), and version VI (f)

3.3. Adopting both methods: segmented PM and modified tooth-tips

The most promising tooth-tips geometries according to the FE analysis presented in Section 3.2 are selected and adopted to the machine with segmented magnets. The model with 4 and 16 magnet segments in the circumferential and axial directions, respectively, is used to explore the impact on W_{PM} and iron loss (P_{Fe}), Table 3.

Table 3. Selected stator tooth-tip design data of the motor having segmented magnet

Motor version	W_{PM} [W]			P_{Fe} [W]			T_e [N·m]	ε [%]	k_T [N·m/A_{rms}]	I [A_{rms}]	k_e [V·s/ rad]	η [-]
	SC	**OC**	**Full load**	**SC**	**OC**	**Full load**	**Full load**			**SC**	**OC**	
Ref. motor	2051	4.94	610	75	212	401	506	16.8	3.38	306	1.89	0.94
Ver. 1 a = 7 mm α = 5°	208	85	153	54	185	355	487	24.3	3.24	328	1.84	0.955
Ver. 2 a = 17 mm α = 7° R = 17 mm	210	67	114	57	169	343	463	34.8	3.09	324	1.85	0.954
Ver. 3 a = 17 mm b = 3 mm	277	75	153	72	185	358	489	22.5	3.26	276	1.77	0.955
Ver. 4 a = 2.15 mm	248	54	80	60	183	317	452	25.1	3.02	278	1.73	0.953
Ver. 5 β = 13°	260	49	91	68	189	345	470	21.6	3.13	281	1.82	0.956
Ver.6 β = 17°	249	56	86	63	180	326	459	28.3	3.06	283	1.75	0.954

Torque constant was reduced up to 12%, and voltage constant (line-to-line) was reduced by 8.5% compared with the values of the reference motor. The proposed machine modifications prove that the W_{PM} can be effectively attenuated by segmenting the magnets with the suggested shape of modified tooth-tips.

4. Conclusion and recommendation

This paper has presented a modified radial-flux machine with PM in order to improve the motor performance. The magnet with a different number of segments in the circumferential and/or axial directions, and the shape of a stator tooth-tip are modified for the purpose of decreasing the magnet eddy-current loss at high rotational speed under AC operation. A parametric study shows that depending on a number of PM segmentation (standard tooth-tip shape) the magnet loss and torque are reduced by 84% and 1.4%, respectively. Other advantages observed are short-circuit current and iron loss reductions. The modified tooth-tip shape (with solid magnet) significantly changes the magnetic path of the armature flux which leads to cut down the magnet loss. The disadvantage is the torque constant and voltage constant reduction. The highest magnet loss and smallest torque/voltage constant reduction are observed in the motor versions III and VI at full load operation (150 A).

From the results of the 3-D and 2-D FEA, it is clear that the proposed modifications to the stator and rotor can significantly reduce the magnet eddy-current loss for a large size machine without significant decreases in torque constant and voltage constant. A high torque ripple and cogging torque are the main disadvantages of the presented modified teeth-tip shapes. To minimize those effects, it is strongly recommended to use the segmented Halbach magnet array, magnetic wedges in the slot and interior-mounted magnets.

Acknowledgements

The authors would like to express their gratitude to the Electrical Machine Laboratory, Department of Electrical & Electronic Engineering, University of Bristol, UK, for supporting the experimental setup for segmented stator thermal tests.

References

[1] Toda H., Xia Z., Wang J., Atallah K., *Rotor eddy-current loss in permanent magnet brushless machines*, IEEE Transactions on Magnetics, no. 4, pp. 2104-2106 (2004).

[2] Lindh P., Nerg J., Pyrhonen J. et al., *Interior permanent magnet motors with non-overlapping concentrated winding or with integral slot winding for traction application*, Przegląd Elektrotechniczny, no. 7b, pp. 9-12 (2012).

[3] EL-Rafeie A.M., Alexander J.P., Calioto S. et al., *Advanced high-power-density interior permanent magnet motor for traction applications*, IEEE Transactions on Industry Application, no. 5, pp. 3235-3248 (2014).

[4] Wang A., Xi W., Wang H. et al., *FEA-based performance calculation of IPM machines with five topologies for hybrid-electric vehicle traction*, Transportation Electrification Asia-Pacific, IEEE Conference and Expo, pp. 1-5 (2014).

[5] Wang J., Juan X., Atallah K., *Design optimization of a surface-mounted permanent-magnet motor with concentrated windings for electric vehicle application*, IEEE Transactions on Vehicular Technology, no. 3, pp. 1053-1064 (2013).
[6] Dutta R., Rahman M.F., *A segmented magnet interior permanent magnet machine with wide constant power range for application in hybrid vehicles*, Vehicle Power and Propulsion, IEEE Conference, Chicago, USA, pp. 7-9 (2005).
[7] Malloy A.C., Mlot A., Cordner M.J., Lamperth M., *Axial flux machines for hybrid module application*, IEEE International Electric Vehicle Conference, Florence, Italy, pp.1-8 (2014).
[8] Aslan T., Semail E., Legranger J., *General analytical model of magnet average eddy-current volume losses for comparison of multiphase PM machines with concentrated winding*, IEEE Transaction, no. 1, pp. 72-83 (2014).
[9] Huang W.Y., Bettayeb A., Kaczmarek R., Vannier J.C., *Optimization of magnet segmentation for reduction of eddy-current losses in permanent magnet synchronous machine*, IEEE Transactions on Energy Conversion, no. 2, pp. 381-387 (2010).
[10] Yamazaki K., Fukushima Y., *Effect of eddy-current loss reduction by magnet segmentation in synchronous motors with concentrated windings*, IEEE Transaction on Industry Applications, no. 2, pp. 779-788 (2011).
[11] Wills D.A., Kamper M.J., *Reducing PM eddy current rotor losses by partial magnet and rotor yoke segmentation*, XIX International Conference on Electrical Machines, pp. 1-6 (2010).
[12] Kawase Y., Ota T., Fukunaga H., *3-D eddy current analysis in permanent magnet of interior permanent magnet motors*, IEEE Transactions on Magnetics, no. 4, pp. 1863-1866 (2014).
[13] Ishak D., Zhu Q., Howe D., *Eddy-current loss in the rotor magnets of permanent-magnet brushless machines having a fractional number of slots per pole*, IEEE Transactions on Magnetics, no. 9, pp. 2462-2469 (2005).
[14] Dajaku G., Gerling D., *A novel tooth concentrated winding with low space harmonic contents*, IEEE International Electric Machines & Drives Conference, Chicago, USA, pp. 755-760 (2013).
[15] Dajaku G., Gerling D., *Eddy current loss minimization in motor magnets of PM machines using high-efficiency 12-teeth/10-slot winding topology*, International Conference on Electrical Machines and Systems, Beijing, China, pp. 1-6 (2011).
[16] Yamazaki K., Kanou Y., Fukushima Y. et al., *Reduction of magnet eddy-current loss in interior permanent-magnet motors with concentrated windings*, IEEE Transactions on Industry Applications, no. 6, pp. 2434-2441 (2010).
[17] Yamazaki K., Ishigami H., *Rotor-shape optimization of interior-permanent-magnet motors to reduce harmonic iron losses*, IEEE Transactions on Industrial Electronics, no. 1, pp. 61-69 (2010).
[18] Nakata T., Takahashi N., Uehara K., *Analysis of magnetic characteristics of brushless DC motor taking into account the distribution of magnetization*, IEEE Transactions on Magnetics, vol. 22, pp: 1084-1086 (1986).